Parametric Instability of Hydrogen-enriched Combustion in High-pressure Conditions

Hosung Byun, Clemence Rubiella, *Hyungrok Do
Seoul National University
Seoul 08826, Republic of Korea

1 Introduction

Hydrogen is regarded as a clean fuel, which is carbon-free. Therefore, power industry has developed hydrogen-powered engines which burn pure hydrogen or hydrogen-blended fuels to mitigate the carbon emission issue of traditional power generation methods. However, thermodynamic properties and combustion characteristics of the hydrogen fuel is quite different from conventional hydrocarbon fuels. Flashbacks due to the faster flame propagation [1], increasing NOx production from the increased flame temperature, and unexpected combustion instability modes from parametric instability [2] should be considered for its practical use. Particularly, the parametric instability is difficult to predict although it can severely limit the operation range of the engines with hydrogen enrichment. In this study, the transient parametric instability is characterized in hydrogen-enriched (0 – 50 %) and high-pressure (up to 10 bar) combustion environments by analyzing pressure signals simultaneously with high-speed chemiluminescence imaging. Strong parametric instability is observed when the hydrogen content in fuel is temporally increased.

2 Experiment setups

High-pressure combustion experiments are conducted in a lab-scale swirl-stabilizing combustor facility (Fig. 1) consisting of thermal mass flow controllers, a combustion chamber, water cooling units, and a back-pressure regulator. Reactant gas, a fuel mixture of hydrogen and methane mixed with air, is delivered to the combustor through a swirler with a swirl number of 1.1. The combustor has a cylindrical quartz inner liner and an outer casing with four quartz windows for optical access as depicted in Figure 1. The flame is stabilized in the quartz liner (D= 38 mm, L= 138 mm) where two dynamic pressure sensors (PCB 112A22) monitor the combustion instability, while the big outer casing with a diameter of 200 mm and a length of around 435 mm attenuates the flame-induced pressure waves. The outer casing serving as a large damper allows for back pressure regulation even with large pressure fluctuations from the flame instability in the inner liner. The pressure regulator is water-cooled to regulate the combustion product gas that is mixed with bypass air injected into the chamber outside of the inner liner. A DSLR camera (Nikon D7500) with a 430 ±25 nm bandpass filter

Correspondence to: hyungrok@snu.ac.kr

captures the flame shape (CH fluorescence profiles) while a high-speed camera (Phantom v2640) with a UV-VIS bandpass filter (335–445 nm) records the time evolution of the flame at 3,000 Hz frame rate.

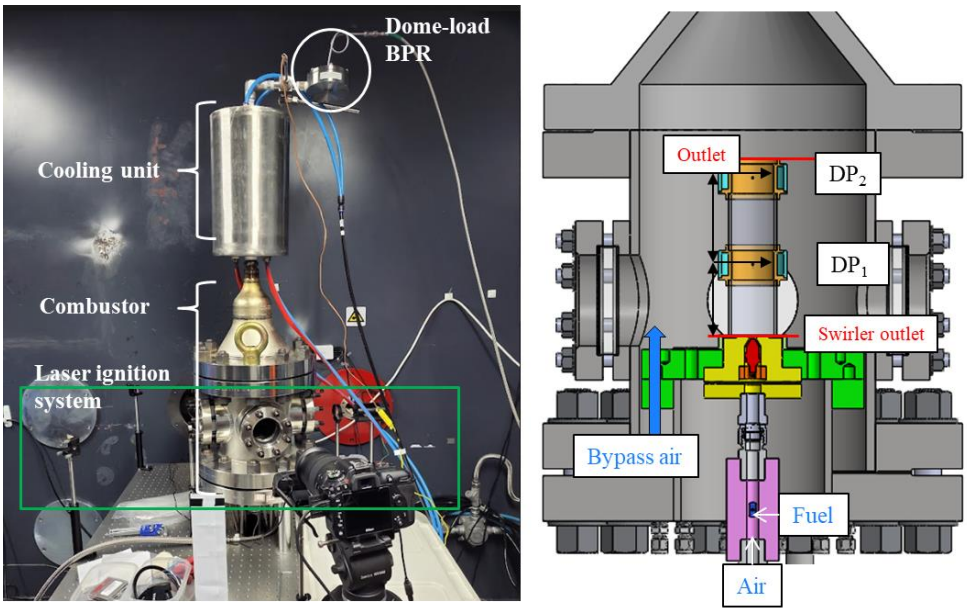

Figure 1: The high-pressure combustion facility (left) and the structure of the combustor (right)

The test conditions are tabulated in Table 1. The fuel equivalence ratio (ϕ) is fixed at 0.8 when the chamber pressure (P) is at 3 bars (S1 and S2) and 5 bars (S3 and S4). S1 and S3 are pure methane combustion cases, and equimolar H_2-CH_4 fuel blend (50 % hydrogen) is injected in S2 and S4. Under the four low pressure conditions, S1 – S4, the flame is well stabilized on the burner. The 'S' of the cases stands for steady fuel conditions and 'T' means transient increment of hydrogen content in fuel blends. In the 'T' cases, the flow rates of H_2 and CH_4 are programmed to gradually raise the H_2 volume % in the fuel blend, 10 % increase per 0.6 second, keeping the overall equivalence ratio unchanged at 0.9. In the high-pressure test conditions (P= 7, 10 bar) with the increasing H_2 content in fuel, T1 – T4, significant transient flame behaviors are observed. The dominant instability frequencies are resolved by water-cooled dynamic pressure sensors (S1 – S4, T1 and T2) and a high-speed camera (T3 and T4).

Table 1: Test conditions and dominant frequencies of combustion instability

Test	CH_4 [nlpm]	H_2 [nlpm]	Air [nlpm]	P [bar]	ϕ	X_{H2} [%]	$\bar{u}_{SI}$ [m/s]	f [Hz]
Steady-state								
S1	5.18	0.0	61.4	3	0.80	0	5.28	1237.0
S2	3.99	4.0	58.8		0.81	50	5.29	1115.7
S3	7.06	0.0	83.8	5	0.80	0	4.32	1232.0
S4	5.39	5.4	80.2		0.80	50	4.33	1144.0
Transient								
T1	10.99	0	116.3	7	0.90	0	4.32	1281.9
	9.93	4.3				30	4.43	1036.5

T2	9.93	4.3			0.90	30	4.43	1023.8
	8.79	8.9				50	4.55	1343.2
T3	10.77	0	113.5	7	0.90	0	4.22	1052.5 1217.4
	8.59	8.7				50	4.44	606.9
T4	15.32	0	162.2	10	0.90	0	4.22	646.9
	12.24	12.4				50	4.44	

3 Result and Discussion

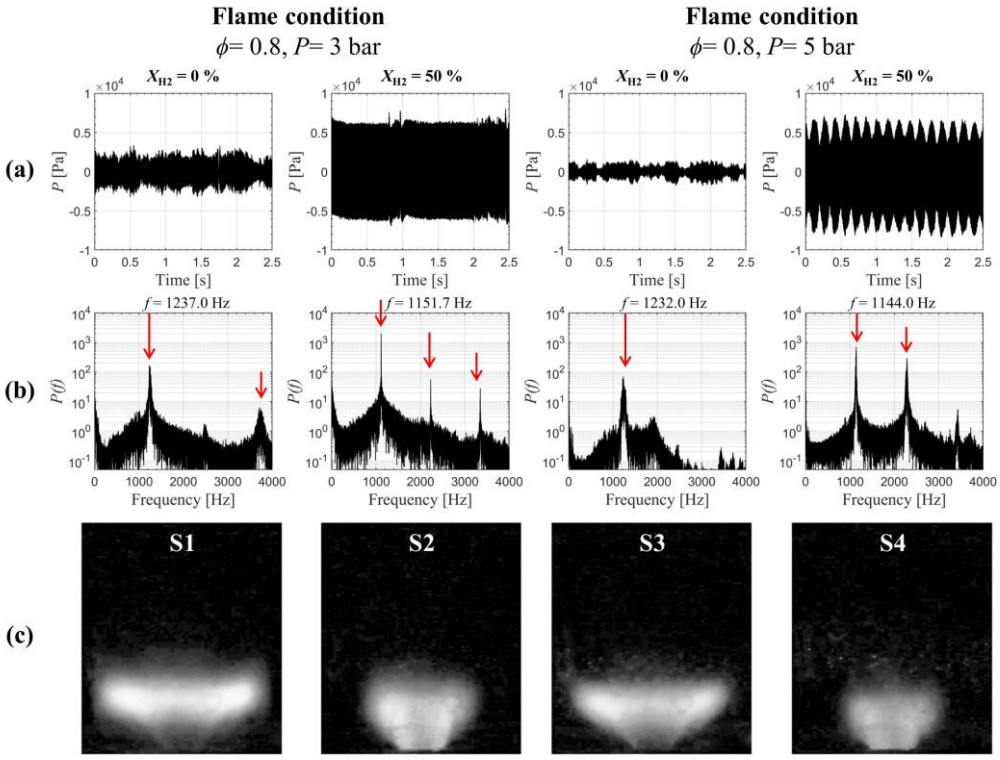

Figure 2: Pressure oscillations shown in (a) time- and (b) frequency-domains, and (c) corresponding flame chemiluminscence images in S1 – S4.

Under the low pressure conditions (S1 – S4), distinct flame characteristics of the pure methane (S1 and 3) and the H_2 fuel blend (S2 and S4) are resolved in Fig. 2. As shown in Fig. 2(c), the CH_4 flame reacts mainly in the shear layer of the recirculation region and therefore, stretches toward the liner wall. However, the hydrogen fuel blend burns near the nozzle exit owing to the hydrogen-enhanced faster chemical reactions, accompanying the stronger pressure oscillation as shown in Fig. 2(a). Recall that the flow speed is much higher near the nozzle exit than in the shear layer. Different flame shapes, e.g., length and angle of the flame cone, imply different flame transfer functions [3]; therefore, not only the fundamental fluctuation frequency changes but also different resonance modes may appear. The pure methane flame generates typical quarter-wave resonance in the open-closed liner geometry (length = 138mm) as shown in Fig. 2(b) of S1. On the other hand, sharper frequency peaks shown in Fig. 2(b) of S2 and S4 in the hydrogen-enriched conditions indicate distinctive instability modes different from the pure methane cases. Interestingly, strong second harmonic frequency peaks which are supposed to be

prohibited for the quarter-wave resonance appear in S2 and S4 unlike in S1 and S3. In other words, the harmonic modes are detected both at odd and even multiples of the fundamental frequency, which is similar to the previously reported 'intrinsic' flame instability [4-5]. This at least clarifies that the hydrogen enrichment alters combustion instability modes.

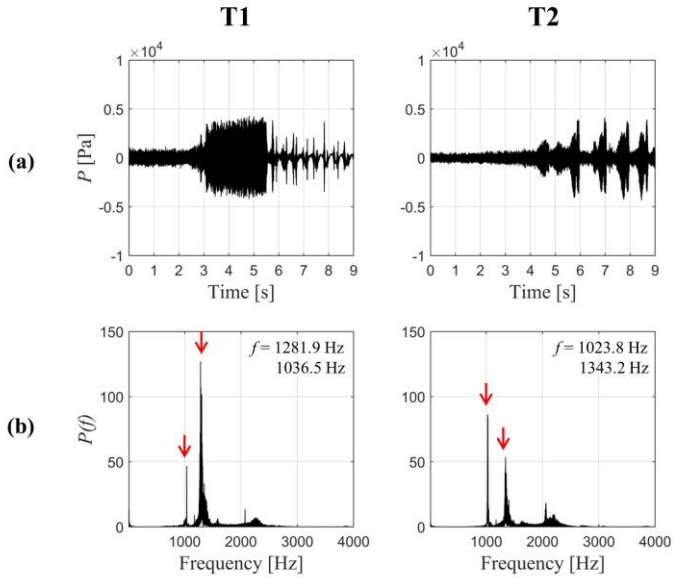

Figure 3: Pressure oscillations recorded in T1 and T2

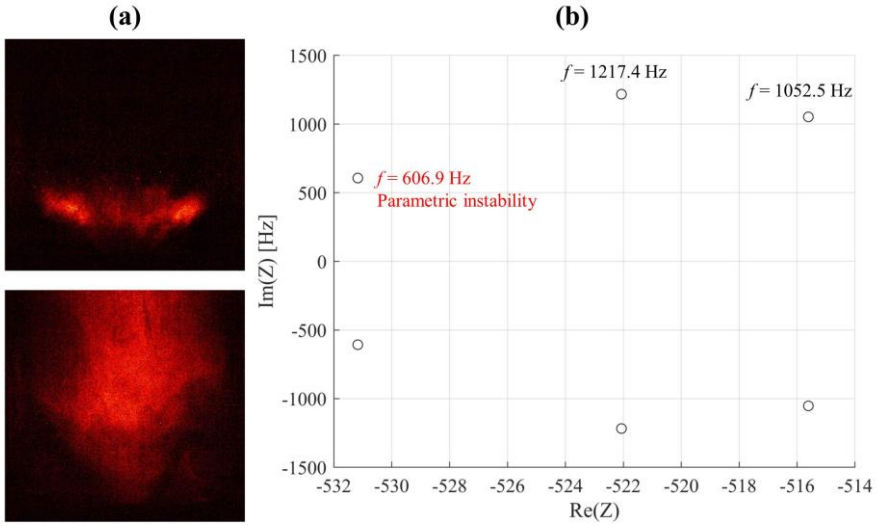

Figure 4: (a) Periodically switching flame shapes and (b) dynamic mode decomposition results of high-speed chemiluminescence images in T3

Figures 3 and 4 reveal that the transient hydrogen addition also affects the combustion instability. Two different types of combustion instability are observed simultaneously. The low-frequency instability mode of the first type begins to appear from around 5.5 s in Fig 3(a), leaving the pressure peaks at a frequency of 1–2 Hz. The two flame shapes alternate: a typical V-shape flame (Fig. 4(a) upper) from/to a large helical vortex structure detached from the nozzle (Fig. 4(a) lower). The high-frequency instability of the second type is observed both in the pressure traces (Fig. 3(a)) and the high-

speed flame chemiluminescence images. The heat release fields, resolved by the chemiluminescence intensity fields, are analyzed to extract the dominant oscillation frequency using dynamic mode decomposition. One of the combustion instability modes is newly found at 606.9Hz, which is called parametric instability that exhibits the dominant frequency at a half of the pumping frequency, 1,217Hz in T3 case. Similarly in T4, a dominant instability, presumably the 'parametric' instability, is detected at 646.9 Hz. Parametric instability appears when the oscillation magnitude exceeds a certain level and is susceptible to low Lewis number that corresponds to hydrogen-enriched conditions [6-7]. This instability mode has been reported with fundamental flames e.g. propagating flames in a tube or flames in atmospheric conditions [2, 6-8], but not in pressurized turbulent conditions. It is important to note that this parametric instability accelerates chemical reactions [8], potentially resulting in excessive heat release, thermal fatigue, and damages to combustors. Varying hydrogen content in the operation of retrofit combustion systems is highly probable in practice since hydrogen supply is yet insufficient and the 'green' hydrogen production from renewable energy resources is inherently sporadic. Therefore, the conditions inducing the parametric instability should be clarified.

In summary, it was confirmed that the hydrogen addition affects the combustion instability in two different situations, 1) hydrogen enrichment in steady state and 2) transient hydrogen addition to the H_2-CH_4 fuel mixture at a constant total equivalence ratio with decreasing CH_4 supply rate accordingly.

1) Hydrogen enrichment (equimolar H_2-CH_4 fuel mixture) accelerated the flame to anchor upstream closer to the nozzle exit of the swirl stabilized burner where the flow is faster. Therefore, the influence of the hydrogen enrichment may vary depending on the combustor and nozzle geometry. The faster flame interacting with the fast combustible mixture flowing through the narrow nozzle exit structure amplified the pressure fluctuations and the strong second harmonic resonance frequency peaks, not appearing with pure methane flames, were observed.

2) It is evident that the transient hydrogen addition triggers significant unsteady fluctuations in the heat release field as well as the pressure time traces. Interestingly, a low frequency (2Hz) periodic switching of the flame structure was observed; a large helical vortex structure from/to a typical V-shape swirl flame. Another newly detected instability mode seen in the heat release field is the parametric instability appearing at the half of the fundamental quarter-wave resonance frequency.

References

[1] An Q, Kheirkhah S, Bergthorson J, Yun S, Hwang J, Lee WJ, Kim MK, Cho JH, Kim HS, Vena P. (2021). Flame stabilization mechanisms and shape transitions in a 3D printed, hydrogen enriched, methane/air low-swirl burner. International Journal of Hydrogen Energy. 46: 14764.

[2] Quinlan JM. (2022). Parametric Combustion Instabilities. AIAA SCITECH 2022 Forum.

[3] Schuller T, Daniel D, and Candel S. (2003). A unified model for the prediction of laminar flame transfer functions: comparisons between conical and V-flame dynamics. Combustion and flame. 134: 21.

[4] Albayrak A, Steinbacher T, Komarek T, Polifke W. (2018). Convective scaling of intrinsic thermo-acoustic eigenfrequencies of a premixed swirl combustor. Journal of Engineering for Gas Turbines and Power. 140: 041510.

[5] Hoeijmakers M, Kornilov V, Arteaga IL, Goey PD, Nijmeijer H. (2014). Intrinsic instability of flame–acoustic coupling. Combustion and Flame. 161: 2860.

[6] Dubey AK, Koyama Y, Hashimoto N, Fujita O. (2019). Experimental and theoretical study of secondary acoustic instability of downward propagating flames: Higher modes and growth rates. Combustion and flame. 205: 316.

[7] Dubey AK, Koyama Y, Hashimoto N, Fujita O. (2021). Acoustic parametric instability, its suppression and a beating instability in a mesoscale combustion tube. Combustion and Flame. 228: 277.

[8] Yoon SH, Noh TJ, Fujita O. (2016). Onset mechanism of primary acoustic instability in downward-propagating flames. Combustion and flame. 170: 1.